

HULL DESIGN CONSIDERATIONS FOR IMPROVED STABILITY OF FISHING VESSELS IN WAVES

Marcelo A. S. NEVES, Department of Naval Architecture and Ocean Engineering, Federal University of Rio de Janeiro, (Brazil)

Nelson A. PÉREZ, Institute of Maritime and Naval Sciences, Austral University, (Chile)
Osvaldo M. LORCA, Bureau Veritas Brazil, (Brazil)

Claudio A. RODRIGUEZ, Department of Naval Architecture and Ocean Engineering, Federal University of Rio de Janeiro, (Brazil)

Abstract

The paper describes an investigation on the relevance of parametric resonance for two typical fishing vessels in head seas. The investigation is aimed at assessing the influence of the incorporation of a transom stern to the design. Results for different Froude numbers are discussed. The first region of resonance is investigated. Distinct metacentric heights and wave amplitudes are considered.

Quite intense resonances are found to occur. These are associated with specific values of metacentric height, ship speed and stern shape. In order to analyse the experimental/numerical results, analytic consideration is given to distinct parameters affecting the dynamic process of roll amplification. The influence of heave, pitch, wave passage effect, speed and roll restoring characteristics are discussed.

1. INTRODUCTION

Parametric resonance of ships in longitudinal regular waves is discussed in the paper, as this is an important particular situation. Results for two typical fishing vessels are compared. Head seas conditions are contemplated in the discussions.

Recently, some papers have called attention to the problem of parametric excitation in head seas. France et al (2001)[1] reported on strong roll amplification in the case of a container ship. Dallinga, Blok and Luth (1998)[2], Luth and Dallinga (1999)[3] reported on the development of head seas parametric resonance in cruise vessels.

A non-linearly coupled mathematical model capable of describing roll parametric amplification in waves is introduced. Emphasis is given on the description of the complete hydrostatic coupling between the heave, roll and pitch modes. The connection between these non-linear hydrostatic coupling terms and the parametric excitation is discussed. The relationship between the main coefficients and some hull characteristics are pointed out.

In order to investigate the influence of speed, fishing vessel roll behaviour is discussed for some velocities and loading conditions leading to parametric resonance. The study then focuses on analysing the influence of speed on the roll motion amplification at the first region



of the stability diagram. An assessment is made of the influence of some relevant parameters directly related to practical aspects of ship design for improved stability.

The two vessels have very similar characteristics but their sterns are different. One is a round stern vessel; the other one has a transom stern. For each hull, two metacentric heights were tested. Additionally, different speeds and wave amplitudes were considered. The transom stern configuration had proved to be responsible for large roll amplifications in the zero speed of advance previously tested case, Neves, Pérez and Valerio (1999)[4]. One relevant question that the present paper intends to answer is whether a transom stern arrangement defines strong parametric resonance when different speeds in head seas are considered. Some conditions show intense amplification. The influence of hull stern shape is discussed. Its influence on the dynamics of roll parametric resonance is shown to be relevant when low metacentric height conditions are considered.

For some tuning conditions the transom stern hull may display at high speeds stronger roll amplifications than those registered in the low speed range. Results are interpreted having into account the main terms affecting the energy balance of coupled modes.

The paper shows that similar hulls tested in similar conditions may display very distinct responses at specific testing conditions. The experiments clearly demonstrate that in some cases strong parametric resonance in head seas can take place in quite few cycles. It is demonstrated that the effect of speed on parametric resonance is strongly dependent on stern shape. A transom stern, incorporating longitudinal asymmetry in flare, may exert a significant influence in establishing the tendency of a fishing vessel hull to display strong parametric amplification in head seas, particularly in a condition of low metacentric

height. These conclusions are relevant in practice for hull design and operational considerations in rough seas.

Finally, the dynamics of motion around one particular tuning frequency is analysed. Considering steady roll responses around the $\omega_e = 2\omega_n$ tuning condition for a given reference speed, it is observed that for speeds slightly lower than this reference speed, due to reduced damping and non-linear restoring characteristics of the hull, roll responses are larger than at the *exact* tuning. It is shown that the roll response curve has a marked asymmetry with respect to the reference speed. Jump effect is identified as a potentially relevant dynamic characteristic to be taken into account in the design of ships subjected to roll parametric amplification.

2. TESTED CONDITIONS

The tests were conducted at the Ship Model Basin of the Austral University, Valdivia, Chile. The tank main dimensions are: 45.0m of total length, 3.0m of breadth and 1.8m of depth. A flap-type wave generator positioned at one extreme of the tank generates regular waves. More details about the towing tank and experimental arrangements may be encountered in [4].

The main characteristics of the ships used in this paper are listed in Table I. Figures 1 and 2 show their lines plans. From Table I and Figs. 1 and 2 it may be observed that the two hulls have very similar dimensions and characteristics but different stern arrangements. The first one will be called RS. It is a quite typical fishing vessel hull form with conventional round stern. The second hull, which will be called TS, corresponds to a typical transom stern fishing vessel. The tested models were built to a scale 1:30. As mentioned previously, the two hulls had

already been tested under parametric resonance in the case of zero speed of advance, [4, 9].

Table I: Principal Particulars of Ships

Denomination	RS	TS
Length (m)	24.36	25.91
Length between perp. (m)	21.44	22.09
Beam (m)	6.71	6.86
Depth (m)	3.35	3.35
Draught (m)	2.49	2.48
Displacement (tons)	162.6	170.3
Waterplane area (m ²)	102.5	121.0
Radius of gyration r_{yy} (m)	5.35	5.52

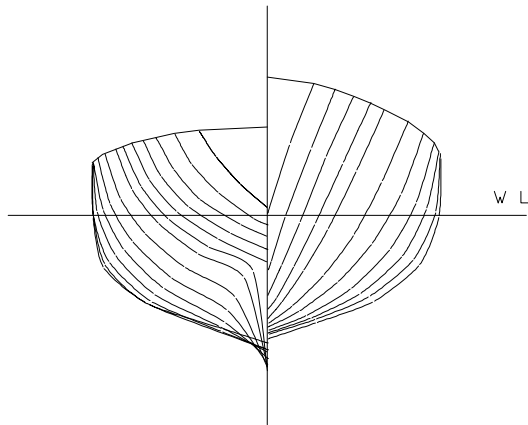


Fig. 1. Body plan of tested vessel RS

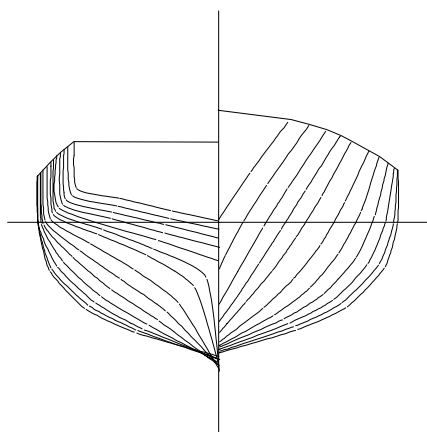


Fig. 2. Body plan of tested vessel TS

In the experiments, the first region of resonance was investigated. This is defined as the condition corresponding to the encounter frequency coinciding with twice the roll natural

frequency, [5, 6]. In other words, the conditions were defined associated with one single encounter frequency $\omega_e = \omega - kU \cos \chi$ for each loading condition.

Table II: Tested Conditions for RS

GM (m)	Fn	λ (m)	a (m)	Wave steepness h_w / λ	$\bar{\phi}$ (deg.)
0.34	0.10	39.0	0.59	1/33	7
			0.69	1/28	14
			0.84	1/23	30
	0.14	43.2	0.51	1/42	3
			0.80	1/27	20
			0.84	1/26	24
	0.20	49.2	0.75	1/33	5
			0.87	1/28	7
			0.96	1/26	17
	0.34	62.4	0.90	1/35	0
			1.02	1/31	5
	0.48	0.10	28.7	0.48	1/30
0.66				1/22	20
0.90				1/16	32
0.14		32.1	0.54	1/30	9
			0.66	1/25	18
			0.90	1/18	30
0.20		37.0	0.48	1/39	5
			0.66	1/28	16
			0.90	1/21	20
0.34		47.8	1.02	1/18	21
			1.02	1/23	0

In the above definition, ω is the wave frequency, U is the ship speed, k is the wave number and χ is the angle of wave incidence with respect to the ship. For head seas, $\chi = 180^\circ$. The tested conditions were those defined in Tables II and III. In these tables, a is wave amplitude, h_w is the wave height and λ is wavelength.

Table III: Tested Conditions for TS

GM (m)	Fn	λ (m)	a (m)	Wave steepness h_w / λ	$\bar{\phi}$ (deg.)
0.37	0.11	31.6	0.30	1/53	15
			0.66	1/24	27
	0.15	35.1	0.45	1/39	18
			1.02	1/17	28
	0.20	39.4	0.45	1/44	4
			0.60	1/33	19
0.30	47.6	0.60	1/40	5	
0.50	0.11	24.5	0.39	1/31	19
			0.63	1/19	22
			1.02	1/12	27
	0.15	27.5	0.39	1/35	2
			0.60	1/23	13
			1.08	1/13	16.5
	0.20	31.2	1.02	1/15	0
	0.30	38.1	1.02	1/19	0

The last columns of Tables II and III present, for each speed and wave amplitude, for the tested conditions corresponding to $\omega_e = 2\omega_n$ (where ω_n is the natural frequency in the roll mode) the registered values of $\bar{\phi}$ (in degrees), the final (steady) roll amplitude observed in each test after all transients had died out. Clearly, for constant encounter frequency, this final roll amplitude is a measure of the level of parametric amplification in each tested condition.

In summary, the experimental test programme involved two hulls with distinct stern arrangements to be compared, each vessel with two metacentric heights, varying speeds and wave amplitudes.

3. EQUATIONS OF MOTION

A *derivative* model is adopted. Following the nomenclature previously used in Neves and

Valerio [7], equations of motion in heave, roll and pitch, with hydrostatic non-linearities up to third order, may be written as:

$$\begin{aligned}
 & (m + Z_{\ddot{z}})\ddot{z} + Z_{z\dot{z}}\dot{z} + Z_{z\ddot{\theta}}\ddot{\theta} + Z_{z\dot{\theta}}\dot{\theta} + Z_{zz}z + Z_{z\theta}\theta + \\
 & + \frac{1}{2!}(Z_{zzz}z^2 + Z_{z\phi\phi}\phi^2 + Z_{z\theta\theta}\theta^2 + 2Z_{z\theta}z\theta) + \\
 & + \frac{1}{3!}(Z_{zzz}z^3 + Z_{z\theta\theta}\theta^3 + 3Z_{z\phi\phi}z\phi^2 + \\
 & + 3Z_{z\theta\theta}z\theta^2 + 3Z_{z\theta}z^2\theta + 3Z_{z\phi\phi}z\phi^2\theta) + \\
 & + Z_{z\eta}(t)z + Z_{\phi\eta}(t)\phi + Z_{\theta\eta}(t)\theta = \\
 & = Z_w(a, \omega_e, \chi) \cos(\omega_e t - \lambda_3) \quad (1)
 \end{aligned}$$

$$\begin{aligned}
 & (J_x + K_{\ddot{\phi}})\ddot{\phi} + K(\dot{\phi}) + K_{\phi\phi}\phi + \frac{1}{2!}(2K_{z\phi}z\phi + 2K_{\phi\theta}\phi\theta) + \\
 & + \frac{1}{3!}(K_{\phi\phi\phi}\phi^3 + 3K_{zz\phi}z^2\phi + 3K_{\phi\theta\theta}\phi\theta^2 + 6K_{z\phi\theta}z\phi\theta) + \\
 & + K_{z\eta}(t)z + K_{\phi\eta}(t)\phi + K_{\theta\eta}(t)\theta = \\
 & = K_w(a, \omega_e, \chi) \cos(\omega_e t - \lambda_4) \quad (2)
 \end{aligned}$$

$$\begin{aligned}
 & (J_y + M_{\ddot{\theta}})\ddot{\theta} + M_{\dot{\theta}}\dot{\theta} + M_{z\ddot{z}}\ddot{z} + M_{z\dot{z}}\dot{z} + M_{zz}z + M_{\theta\theta}\theta + \\
 & + \frac{1}{2!}(M_{zzz}z^2 + M_{z\phi\phi}z\phi^2 + M_{z\theta\theta}z\theta^2 + 2M_{z\theta}z\theta) + \\
 & + \frac{1}{3!}(M_{zzz}z^3 + M_{z\theta\theta}z\theta^3 + 3M_{z\phi\phi}z\phi^2 + \\
 & + 3M_{z\theta\theta}z\theta^2 + 3M_{z\theta}z^2\theta + 3M_{z\phi\phi}z\phi^2\theta) + \\
 & + M_{z\eta}(t)z + M_{\phi\eta}(t)\phi + M_{\theta\eta}(t)\theta = \\
 & = M_w(a, \omega_e, \chi) \cos(\omega_e t - \lambda_5) \quad (3)
 \end{aligned}$$

On the right hand side of these equations, Z_w , K_w , M_w describe the amplitude of wave external excitation in the heave, roll and pitch modes, respectively, whereas λ_3 , λ_4 , λ_5 are their corresponding phase lags with respect to the waves. In the left hand side of the equations, non-linear restoring terms include dependence on all body modes (z, ϕ, θ) and wave passage (η). Dots refer to velocities; double dots to accelerations. In all modes,

coefficients with dotted and double dotted subscripts are damping and added masses coefficients, respectively.

A set of linear equations with time-dependent coefficients is obtained when the variational equations are obtained. Defining the motions as:

$$\begin{aligned} z(t) &= \hat{z}(t) + \xi(t) = z_a \cos(\omega_e t + \alpha_z) + \xi(t) \\ \phi(t) &= \hat{\phi}(t) + \varphi(t) = \phi_a \cos(\omega_e t + \alpha_\phi) + \varphi(t) \quad (4) \\ \theta(t) &= \hat{\theta}(t) + \vartheta(t) = \theta_a \cos(\omega_e t + \alpha_\theta) + \vartheta(t) \end{aligned}$$

where $\xi(t), \varphi(t), \vartheta(t)$ are perturbations superposed to the steady solutions $\hat{z}, \hat{\phi}, \hat{\theta}$, then, inserting expressions (4) into equations (1), (2) and (3), the equations of motion relative to the perturbed motions become:

$$\begin{aligned} (m + Z_{\dot{z}}) \ddot{\xi} + Z_{z\dot{z}} \dot{\xi} + Z_{z\ddot{\theta}} \ddot{\theta} + Z_{z\dot{\theta}} \dot{\theta} + Z_{z\xi} \xi + Z_{z\vartheta} \vartheta + \\ + (Z_{zz\hat{z}} + Z_{z\theta\hat{\theta}} + \frac{1}{2} Z_{zzz} \hat{z}^2 + \\ + \frac{1}{2} Z_{z\phi\hat{\phi}} \hat{\phi}^2 + \frac{1}{2} Z_{z\theta\hat{\theta}} \hat{\theta}^2 + Z_{zz\theta} \hat{z} \hat{\theta}) \xi + \\ + (Z_{\phi\phi\hat{\phi}} \hat{\phi} + Z_{z\phi\hat{\phi}} \hat{z} \hat{\phi} + Z_{\phi\phi\theta} \hat{\phi} \hat{\theta}) \varphi + \\ + (Z_{z\theta\hat{z}} + Z_{\theta\theta\hat{\theta}} + \frac{1}{2} Z_{zz\theta} \hat{z}^2 + \\ + \frac{1}{2} Z_{\phi\phi\theta} \hat{\phi}^2 + \frac{1}{2} Z_{\theta\theta\theta} \hat{\theta}^2 + Z_{z\theta\theta} \hat{z} \hat{\theta}) \vartheta + \\ + Z_{z\eta}(t) \xi + Z_{\varphi\eta}(t) \varphi + Z_{\theta\eta}(t) \vartheta = 0 \quad (5) \end{aligned}$$

$$\begin{aligned} (J_x + K_{\ddot{\phi}}) \ddot{\varphi} + K_{\phi\dot{\phi}} \dot{\varphi} + K_{\phi\ddot{\theta}} \ddot{\theta} + K_{\phi\varphi} \varphi + \\ + (K_{z\phi\hat{\phi}} \hat{\phi} + K_{zz\phi} \hat{z} \hat{\phi} + K_{z\phi\theta} \hat{\phi} \hat{\theta}) \xi + \\ + (K_{z\phi\hat{z}} + K_{\phi\theta\hat{\theta}} + \frac{1}{2} K_{\phi\phi\phi} \hat{\phi} + \\ + \frac{1}{2} K_{zz\phi} \hat{z}^2 + \frac{1}{2} K_{\phi\theta\theta} \hat{\theta}^2 + K_{z\phi\theta} \hat{z} \hat{\theta}) \varphi + \\ + (K_{\phi\theta\hat{\phi}} \hat{\phi} + K_{\phi\theta\theta} \hat{\theta} + K_{z\phi\theta} \hat{z} \hat{\theta}) \vartheta + \\ + K_{z\eta}(t) \xi + K_{\varphi\eta}(t) \varphi + K_{\theta\eta}(t) \vartheta = 0 \quad (6) \end{aligned}$$

$$\begin{aligned} (J_y + M_{\ddot{\theta}}) \ddot{\vartheta} + M_{\theta\dot{\theta}} \dot{\vartheta} + M_{z\ddot{\xi}} \ddot{\xi} + M_{z\dot{\xi}} \dot{\xi} + M_{z\xi} \xi + M_{\theta\vartheta} \vartheta + \\ + (M_{zz\hat{z}} + M_{z\theta\hat{\theta}} + \frac{1}{2} M_{zzz} \hat{z}^2 + \\ + \frac{1}{2} M_{z\phi\hat{\phi}} \hat{\phi}^2 + \frac{1}{2} M_{z\theta\hat{\theta}} \hat{\theta}^2 + M_{zz\theta} \hat{z} \hat{\theta}) \xi + \\ + (M_{\phi\phi\hat{\phi}} \hat{\phi} + M_{z\phi\hat{\phi}} \hat{z} \hat{\phi} + M_{\phi\phi\theta} \hat{\phi} \hat{\theta}) \varphi + \\ + (M_{z\theta\hat{z}} + M_{\theta\theta\hat{\theta}} + \frac{1}{2} M_{zz\theta} \hat{z}^2 + \\ + \frac{1}{2} M_{\phi\phi\theta} \hat{\phi}^2 + \frac{1}{2} M_{\theta\theta\theta} \hat{\theta}^2 + M_{z\theta\theta} \hat{z} \hat{\theta}) \vartheta + \\ + M_{z\eta}(t) \xi + M_{\varphi\eta}(t) \varphi + M_{\theta\eta}(t) \vartheta = 0 \quad (7) \end{aligned}$$

Equations (5), (6), (7) form a set of time-dependent coupled equations, assumed to regulate, to first approximation, the stability of the dynamic system defined by the non-linear equations defined previously, equations (1), (2) and (3).

4. ROLL INSTABILIZATION

In the case of longitudinal waves, roll motions will not be externally excited, thus $\hat{\phi} \equiv 0$. The roll variational equation may then be expressed as:

$$\begin{aligned} (J_x + K_{\ddot{\theta}}) \ddot{\vartheta} + K_{\theta\dot{\theta}} \dot{\vartheta} + K_{\theta\varphi} \varphi + \\ + (K_{z\theta\hat{z}} + K_{\phi\theta\hat{\theta}} + \frac{1}{2} K_{zz\theta} \hat{z}^2 + \frac{1}{2} K_{\phi\theta\theta} \hat{\theta}^2 + K_{z\phi\theta} \hat{z} \hat{\theta}) \varphi + \\ + K_{\theta\eta}(t) \vartheta = 0 \quad (8) \end{aligned}$$

In this equation, the coefficients associated with parametric excitation are related to derivatives of geometric characteristics of the waterplane area:

$$\begin{aligned} K_{z\phi} &= \frac{\partial I_{xx}}{\partial z}; K_{\phi\theta} = \frac{\partial I_{xx}}{\partial \theta}; K_{zz\phi} = \frac{\partial^2 I_{xx}}{\partial z^2}; \\ K_{z\phi\theta} &= \frac{\partial^2 I_{xx}}{\partial z \partial \theta}; K_{\phi\theta\theta} = \frac{\partial^2 I_{xx}}{\partial \theta^2} \end{aligned}$$

which, in turn, are dependent on the longitudinal distribution of breadth and flare of the hull [7]. The following expressions may be derived:

$$\begin{aligned}
 K_{z\phi} &= \frac{\partial I_{xx}}{\partial z} = -2 \int y^2 \frac{\partial y}{\partial z} dx \\
 K_{\phi\theta} &= \frac{\partial I_{xx}}{\partial \theta} = 2 \int xy^2 \frac{\partial y}{\partial z} dx \\
 K_{zz\phi} &= \frac{\partial^2 I_{xx}}{\partial z^2} = 4 \int y \left(\frac{\partial y}{\partial z} \right)^2 dx + A_0 \\
 K_{z\phi\theta} &= \frac{\partial^2 I_{xx}}{\partial z \partial \theta} = -4 \int xy \left(\frac{\partial y}{\partial z} \right)^2 dx - A_0 x_{f0} \\
 K_{\phi\theta\theta} &= \frac{\partial^2 I_{xx}}{\partial \theta^2} = 4 \int x^2 y \left(\frac{\partial y}{\partial z} \right)^2 dx + I_{yy0}
 \end{aligned} \tag{9}$$

Equation (8), the time-dependent equation describing parametric amplification of the roll motion (to third order), which contains contributions from the heave and pitch motions and the wave passage effect, may be cast in the form of a Hill's differential equation:

$$\begin{aligned}
 \ddot{\phi} + b\dot{\phi} + c_1\phi + \\
 [c_2 \cos(\omega_e t + \alpha_2) + c_3 \cos(\omega_e t + \alpha_3)]\phi = 0
 \end{aligned} \tag{10}$$

It is pointed out that the time-varying terms are a compound result of volumetric changes in the submerged part of the hull due to the heave and pitch motions and the cyclic passage of the longitudinal progressive wave along the hull.

It is well known that this type of equation may have strong instabilities at encounter frequencies close to $\omega_e = 2\omega_n$, where the roll natural frequency, squared, is defined as:

$$\omega_n^2 = \frac{K_\phi}{J_x + K_\phi}$$

see [5, 6]. In the following sessions, the influence of speed on this problem will be discussed for $\omega_e = 2\omega_n$ and near it.

5. VERTICAL MOTIONS

Figs. 3 to 6 present the computed heave and pitch linear responses (amplitude and phase) in the frequency domain for the two hulls. The tested frequencies are indicated by vertical dotted lines. It is observed that the heave responses, Figs. 3 and 4, are practically the same, for zero speed and all other speeds tested. As expected, higher responses are obtained for higher speeds.

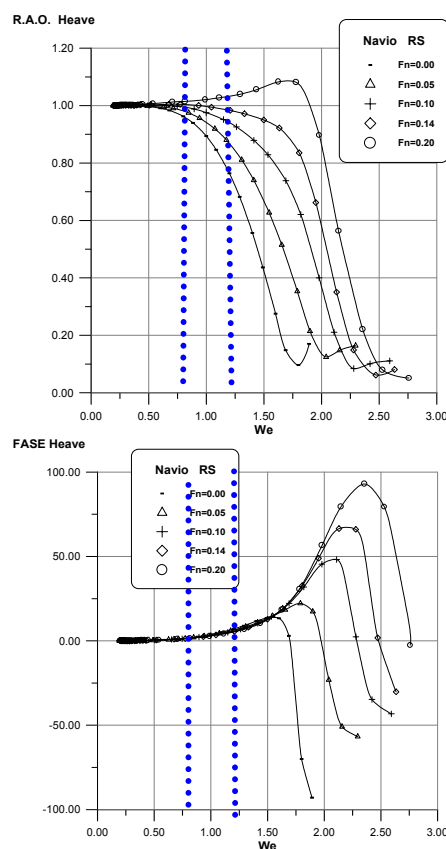


Fig. 3. Heave transfer functions, RS hull.

For the pitch mode, Figs. 5 and 6, some characteristics become apparent. First of all, we note that for zero speed the two hulls respond in practically identical conditions. As speed increases, the responses become distinct. It

may be observed that for the RS hull the pitch amplitudes have a general trend to increase with speed.

In the case of the TS hull, there is a much more limited increase of the pitch amplitudes with speed. It is apparent, then, that if in the zero speed case the two hulls would show similar levels of internal excitation, as speed increases the RS hull would have to cope with higher levels of internal excitation due to the vertical motions.

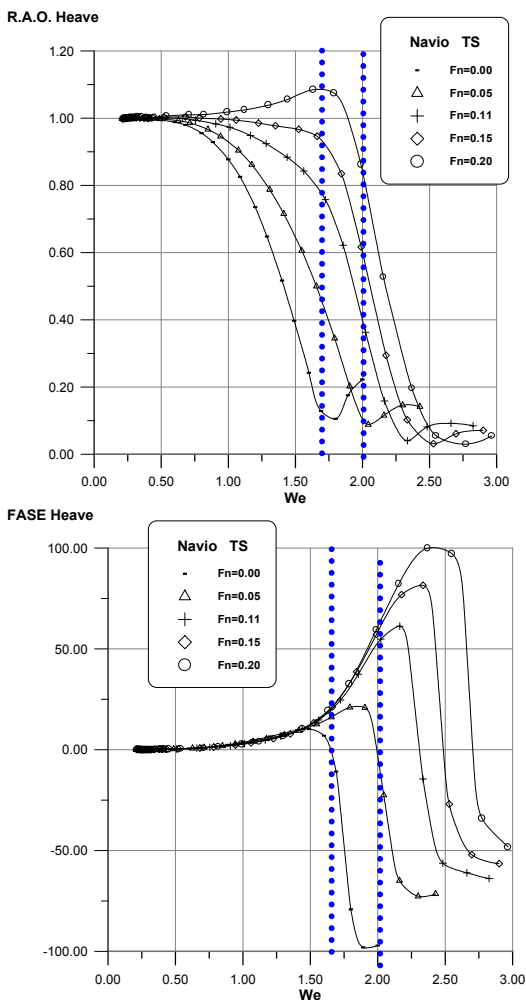


Fig. 4. Heave transfer functions, TS hull.

Yet, as will be made clear below, due to hull characteristics, this is not strictly the case.

Another relevant aspect is that the influence of speed is effective not only in inducing a

compounded effect on the amount of parametric excitation being transferred from the wave excited vertical motions to the rolling motion. It should also be taken into account that as different levels of internal excitation are fed into the dynamic system, there is also a higher level of damping incorporated into the process, its main mechanism being lift damping due to the higher speed. In fact, ship speed tends to (nonlinearly) reduce eddy damping and add (linear) lift damping, [8].

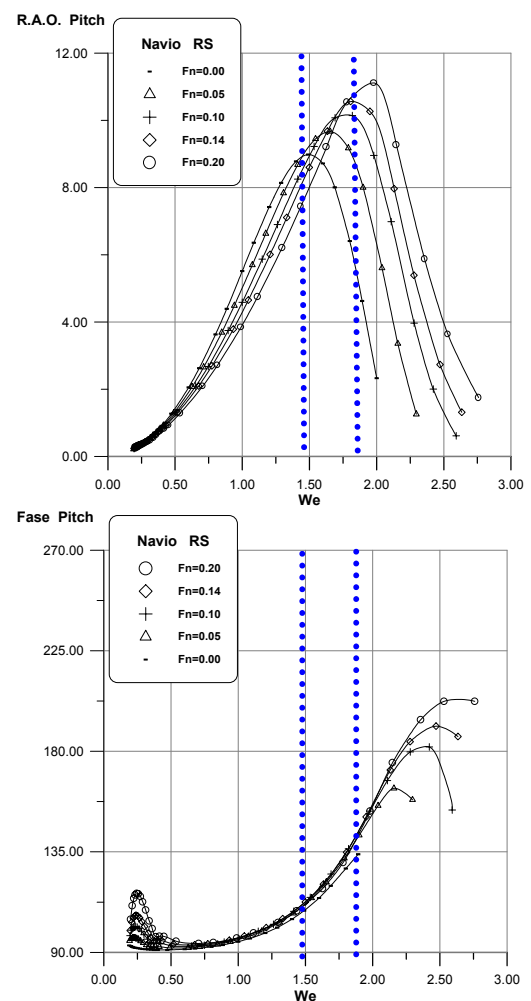


Fig. 5. Pitch transfer functions, RS hull.

The net effect of speed on the balance of internal transfer of energy versus damping is not evident at all, and should be in any case carefully investigated. This observation leads to important considerations directly related to



practical aspects of ship design for improved stability.

At this stage, it is important to note that the RS hull is less damped than the TS hull. This was demonstrated by the roll decrement tests (conducted for the zero speed case). This may be observed in Fig. 7, in which the following non-dimensional parameters are defined:

$$\delta = \omega_e \sqrt{\frac{L}{g}} - \text{non-dimensional frequency.}$$

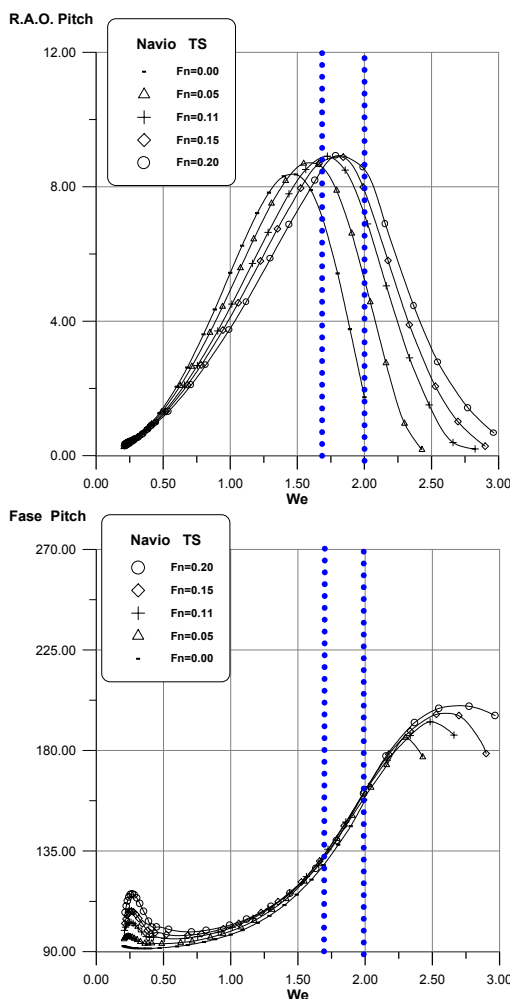


Fig. 6. Pitch transfer functions, TS hull.

$$B'_{44} = \frac{B_{44}}{\rho \left(\frac{L}{2}\right)^5} - \text{non-dimensional roll damping}$$

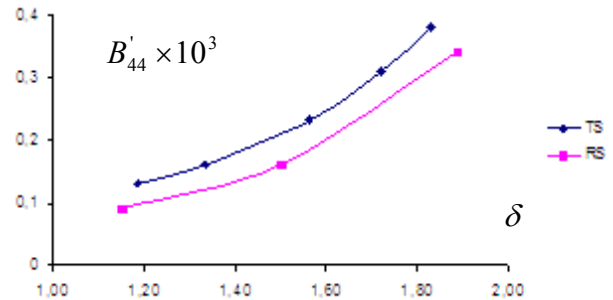


Fig. 7. Equivalent damping at zero speed.

6. RESULTS FOR RS HULL

Considering the results given in Table II, it is observed that for both values of GM and for each Fn there is a linear tendency in the growth of the roll amplitude for larger wave amplitudes. Additionally, this tendency is kept almost the same as larger speeds are considered. There is a clear tendency, when the same wave amplitude is considered, for roll amplitudes to become smaller at higher speeds. Figure 8 illustrates this tendency. The figure displays time series of roll motion obtained for RS, $GM = 0.48m$ for three Froude numbers and $a=0.90m$. Clearly, there is a marked reduction in roll amplification as speed increases. It is noted that for this value of metacentric height no roll amplification was observed for $Fn = 0.34$. The implication here is that with increased speed of advance, more damping (mainly lift damping) now acts against a higher level of vertical motions, but resulting in less roll parametric amplification. Fig. 9 shows how internal in the unstable zone of stability diagram the corresponding tested conditions for $Fn = 0.10$ are.

Another way of viewing this roll reduction with speed is seen in Fig. 10(a,b). In this figure, final (steady) roll amplitudes are plotted

against Froude number for a particular wave amplitude.

For the lower metacentric height condition, Fig. 10(a), the tested wave amplitudes are not exactly the same for all speeds, thus linear interpolation has been adopted. But the important aspect to be observed from the two graphs is the common tendency for roll motion amplification to attenuate in face of higher speeds, irrespective of the tuning.

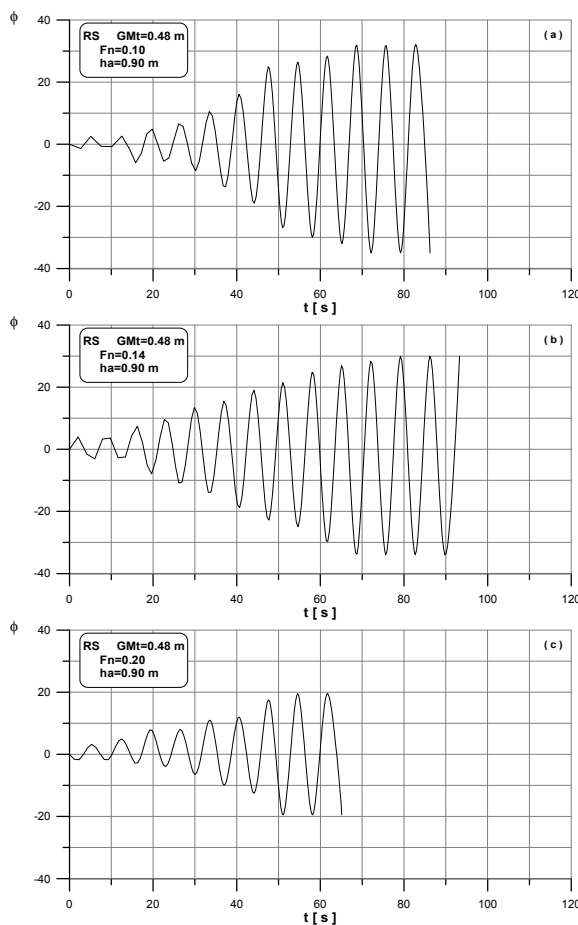


Fig. 8 - Time series of roll motion for RS hull, $GM = 0.48m$, $a = 0.90m$, (a) $Fn = 0.10$; (b) $Fn = 0.14$ and (c) $Fn = 0.20$, respectively.

7. RESULTS FOR TS HULL

Consider now the results for TS hull given in Table III. It may be observed that for the lower

GM and small Froude numbers there is a tendency for roll angles to change in a similar way as discussed previously to the RS hull. Yet, for higher speeds, the tendency is reversed, and it is observed that very large roll angles are obtained for $Fn=0.30$.

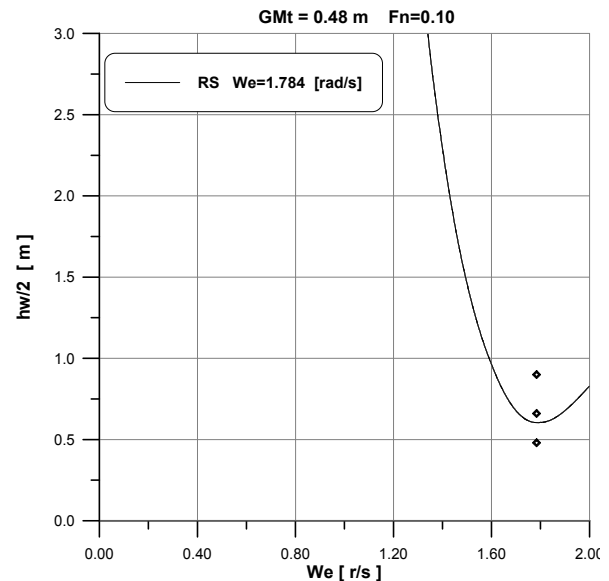


Fig 9 Illustrates how internal the points are for $Fn = 0.10$.

In fact, considering the complete test program, the largest roll response was obtained for this condition, corresponding to angles of the order of 38 degrees being reached in few cycles, wave amplitude being $a=0.78m$. This intense resonance for $Fn=0.30$ is larger than the roll amplitudes registered for zero speed, as reported in [4] and [9]. For zero speed, in less favourable conditions ($GM=0.35m$ and $a=0.90m$), roll angles of 34 degrees were obtained. Still considering this low GM for TS testing, it is observed that at $Fn=0.20$ there are intense responses, though not as intense as in the $Fn = 0.30$ case. For the higher metacentric height, $GM=0.50m$, a tendency similar to what was observed for the RS hull is back: higher speeds now imply lower amplifications. It may be noticed that for TS hull at this high GM condition, for $Fn>0.15$ practically no amplification was observed.

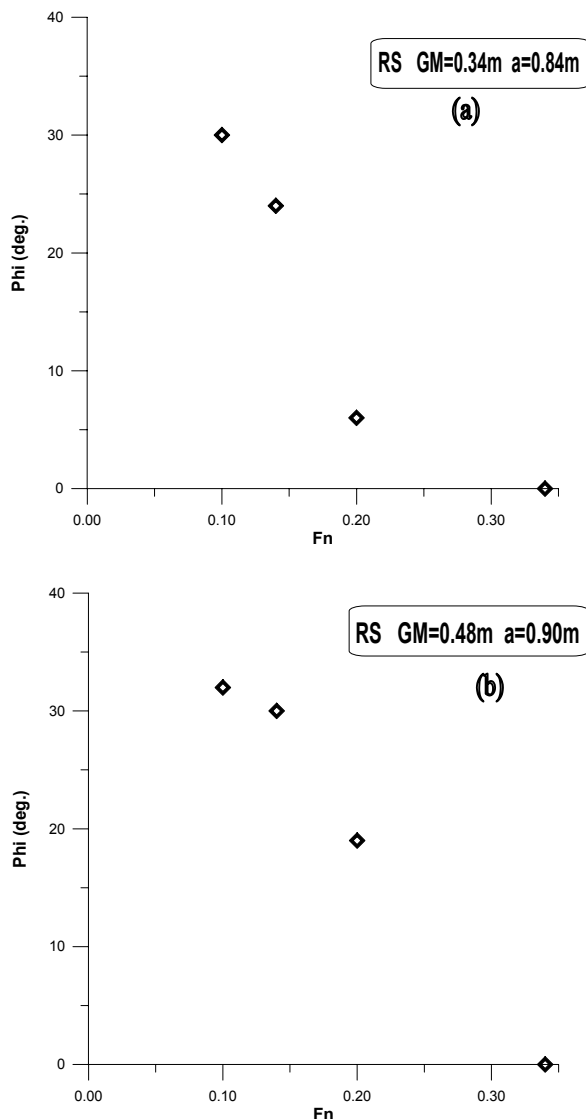


Fig. 10. Roll amplitudes against F_n for RS hull:
(a) $GM = 0.34m$, $a = 0.84m$,
 $\omega_e = 1.49rad/s$; (b) $GM = 0.48m$,
 $a = 0.90m$, $\omega_e = 1.78rad/s$

It may be observed that the situation for TS hull at the low GM condition is completely different from the RS hull responses in the high-speed range. Interpolating in Table III for the lower Froude numbers one gets Fig. 11(a).

When the same procedure is applied in the case of higher GM , for $a=1.02m$, one gets Fig. 11(b).

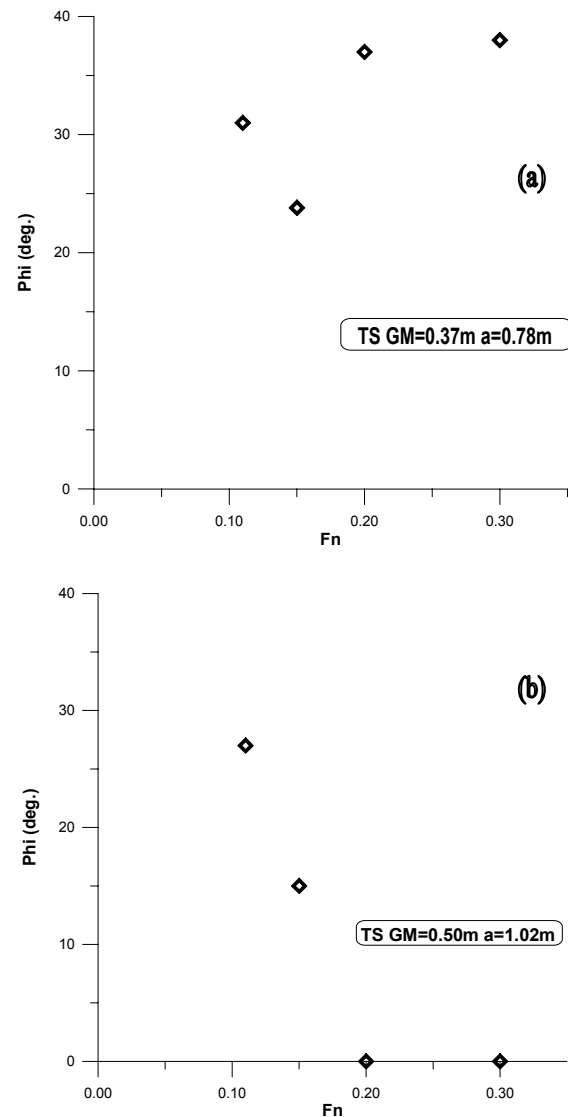


Fig. 11. Roll amplitudes against F_n for TS hull:
(a) $GM = 0.37m$, $a = 0.78m$,
 $\omega_e = 1.72rad/s$; (b) $GM = 0.50m$,
 $a = 1.02m$, $\omega_e = 2.00rad/s$

It is seen in Fig. 11(a) that for TS hull in the range of low speeds corresponding to $0.11 \leq F_n \leq 0.15$, roll amplitudes decay, as was the case with RS hull. But for higher speeds, instead of progressively lower responses, there is now an increase in roll response. In fact, responses are all high, but what is striking is the difference in trend. Now, it is seen that for the higher metacentric height $GM=0.50m$, Fig. 11(b), there is the same previous trend for roll

amplitudes to decay with increased speeds. In fact, for $Fn=0.20$ and above this value, no amplification was observed for this condition.

One notices at first that the TS hull form is in general a more damped hull form than the RS hull, see Fig. 7. Secondly, it is noticed that reports in general point to less parametric amplification in head seas with speed, [1]. This is the observed trend in the present investigation for the RS hull in the two tested loading conditions. It is also the situation with the TS hull at the high metacentric height condition, $GM=0.50m$. What would be the explanation for the distinct trend for TS hull for the low GM condition?

Given the couplings of the modes and the terms in the Hill's equation, expressions (9) and equation (10), it may be concluded that the internal transfer of energy from the vertical modes to the roll motion is regulated essentially by hull form parameters such as the longitudinal distribution of local breadth $b(x)$

and flare at waterline $\left. \frac{dy}{dz} \right|_0(x)$.

It is shown in Fig. 12 that TS hull, due to its transom stern configuration displays much larger longitudinal asymmetry in flare distribution than the RS hull. Thus it is clearly a more efficient converter of energy from vertical modes to roll motion. In this context, it may be argued that for such critical dynamic characteristic to take place, metacentric height must be low. If this is not the case, then increased damping at high speeds will prevail against the unstabilizing effect of parametric excitation.

In summary, low GM ($GM=0.37m$) for transom stern TS hull produces intense parametric resonances at all speeds at wave amplitudes of the order of $a=0.78m$. The other hull, which is less damped, even at a slightly lower metacentric height, $GM=0.34m$, and

larger wave amplitude, $a=0.90m$, tends to respond less and less for higher speeds.

The same TS hull for a high GM condition ($GM=0.50m$) does not amplify parametric excitation at high speeds, indicating that a transom stern shape together with a low GM has a relevant effect on parametric amplification.

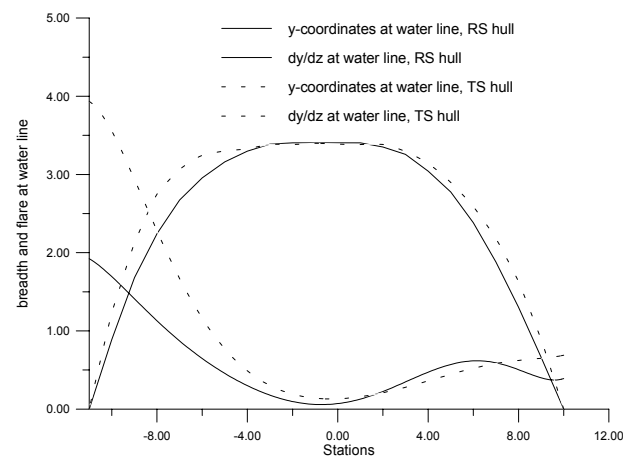


Fig. 12. Longitudinal distribution of breadth and flare at waterline for the two hulls.

8. ROLL RESPONSES AROUND A GIVEN TUNING CONDITION

In the preceding sections the responses of roll motion in parametrically excited conditions have been examined. In all cases, for each metacentric height, as speed was modified, the ratio of the encounter frequency to the roll natural frequency remained the same, always corresponding to $\omega_e = 2\omega_n$. In practice, it meant that in each case, for higher Froude numbers, longer waves excited the hull in the resonant condition. Different wave amplitudes allowed the analysis of the responses in a *vertical* sense in the stability diagrams, see Figure 9. In other words, the previous analysis is related to the investigation of speed effect on the tuning $\omega_e = 2\omega_n$ for a fixed metacentric height condition.

It will be the next step to complementarily examine roll responses in parametric resonance when one single wave is considered (defining the tuning $\omega_e = 2\omega_n$) and distinct speeds are simulated, thus considering hull responses above and below one given tuning condition.

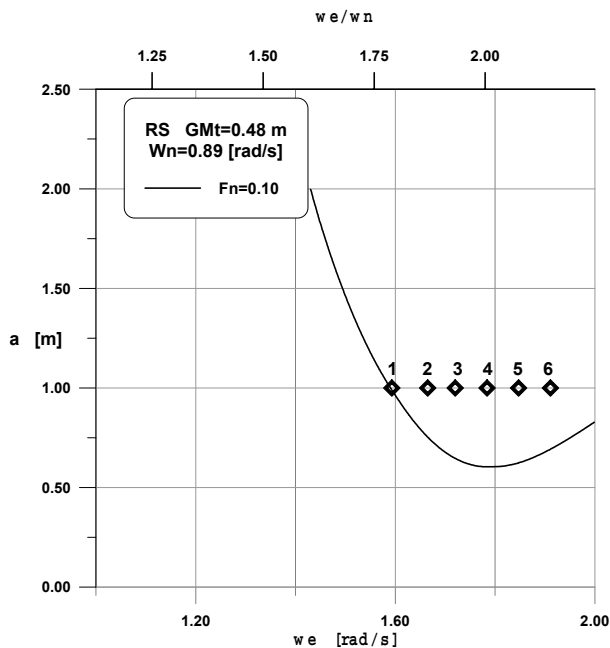


Fig. 13. Points corresponding to different speeds plotted in the stability diagram for $F_n=0.10$.

In this sense, different speeds give the responses in a *horizontal* sense in the stability diagrams, see Fig. 13. For the present purpose the $F_n=0.10$ condition will be examined. Thus, the condition reported in Fig. 8(a) will be taken as reference for an assessment of the amplification of roll motion when ship speed is lower or higher than the one defining the *exact* tuning $\omega_e = 2\omega_n$. Clearly, for the same wave, different speeds will define distinct values for the tuning ratio $\frac{\omega_e}{\omega_n}$. Considering the limits of stability corresponding to Fig. 9, defined in terms of wave amplitude against encounter frequency, points corresponding to different ship speeds in the same wave conditions (wave amplitude and length) will appear as indicated in Fig. 13. Numbered points represent six

different conditions (speeds) in head seas, in a wave with amplitude $a = 1.0$ m and frequency $\omega = 1.46$ rad/s. For clarity, a second horizontal scale is displayed in the upper part of the figure, showing the ratio $\frac{\omega_e}{\omega_n}$. One observes

that point number 4 corresponds to the tuning $\omega_e = 2\omega_n$.

Time series obtained from numerical integration for constant conditions and varying speeds were analysed and the steady roll amplitudes (after transients) were plotted in a non-dimensional roll diagram in Fig. 14, that is, $\frac{\bar{\phi}}{ka}$ versus $F_n = \frac{U}{\sqrt{gL}}$. Therefore, roll

amplitudes corresponding to the numbered points of Fig. 13 may be observed in Fig. 14, plotted against a scale of Froude numbers. So, again, point number 4 corresponds to the $F_n=0.10$ condition, defining the *exact* tuning. It is seen that for very low speeds, corresponding to large detunings, the result is no roll amplification. Point 1 is in this category. Analogously, point 6 is a case of no roll amplification at the high-speed side. Maximum amplification in the response diagram takes place for $F_n=0.07$, between points 2 and 3. Roll amplification at the *exact* tuning is of the order of $\frac{3}{4}$ of the maximum amplification. There is a marked asymmetry in the response diagram. For speeds corresponding to $F_n < 0.065$ (to the left of point 2) there is the appearance of jump effect, with abrupt changes in roll amplitude, from large to very small roll amplitudes.

On the other hand, the right hand side of the response curve displays a smooth reduction in amplitude as speed increases with corresponding larger detuning. Clearly, for all the other conditions related to the other tuning conditions tested, for instance, $F_n=0.14$, $F_n=0.20$, etc, similar curves will be obtained. Time series corresponding to conditions between points 1 and 2 effectively may display

instabilities associated with jump phenomenon, as may occur in dynamic systems mathematically represented by the so-called externally excited Duffing equation. Yet, it is pointed out that the excitation in the present case is in effect an internal transfer of energy from the vertical modes to the roll mode, with speed effects as discussed in the previous session on the components of parametric excitation.

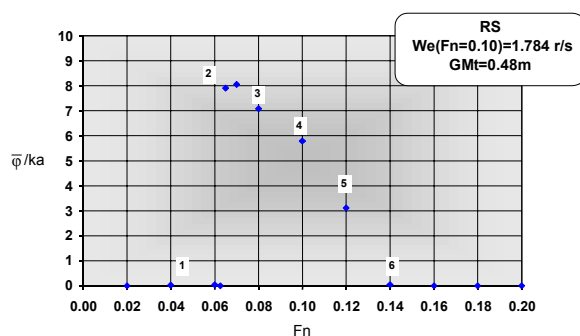


Fig. 14. non-dimensional steady roll responses ($\frac{\bar{\phi}}{ka}$) for different Froude numbers.

9. CONCLUSIONS

A third order coupled non-linear mathematical model in the restoring modes was presented. The time-dependent linear equations defining the stability of the non-linear system were also given.

Results of a series of experiments on parametric rolling undertaken for two fishing vessels in head seas have been presented. The first region of Mathieu instability was investigated. The parameters varied in the test programme were: wave amplitudes, metacentric heights, and speeds.

Similar hulls tested in similar conditions displayed very distinct responses at specific testing conditions. The experiments demonstrate that in some cases strong parametric resonances in head seas can take place in quite few cycles. Angles of the order

of 38 degrees have been reached for wave conditions often met by fishing vessels at sea. This is indicative that for this type of vessel, head seas conditions may be a source of real risk of ship capsize.

The effect of speed on parametric resonance is strongly dependent on stern shape. A transom stern design, usually incorporating longitudinal asymmetry in the flare distribution, may exert a significant influence in establishing the tendency of a fishing vessel hull to display strong parametric amplification in head seas, particularly in a condition of low metacentric height.

These conclusions are relevant in practice for hull design and operational considerations in rough seas. If a longitudinal distribution of flare is considered as a design solution, then proper account of the potentially higher parametric excitation should be given. It is pointed out that, as shown in the analysis, an increase in metacentric height is a possible via of solution to the problem, but this is not always available for some vessel types. This is clearly the situation with typical fishing vessels.

Finally, considering steady roll responses around a given speed corresponding to the $\omega_e = 2\omega_n$ condition, it is observed that for speeds slightly lower than this reference speed, due to reduced damping and non-linear restoring characteristics of the hull, roll responses are larger than at the *exact* tuning. The response curve has a marked asymmetry with respect to the reference speed. Jump effect may be an associated dynamic feature in a roll amplification phenomenon due to parametric resonance.

10. ACKNOWLEDGEMENT

This work was partially supported by CNPq and FAPERJ of Brazil and CONICYT of Chile.



The authors express their thanks for this financial support.

11. REFERENCES

- [1] France, W. N.; Levadou, M.; Treacle, T. W.; Paulling, J. R.; Michel, R. K.; Moore, C. (2001), "An Investigation of Head-Sea Parametric Rolling and its Influence on Container Lashing Systems". SNAME Annual Meeting.
- [2] Dallinga, R. P.; Blok, J. J.; Luth, H. R. (1998), "Excessive Rolling of Cruise Ships in Head and Following Waves". RINA International Conference on Ship Motions & Manoeuvrability, London, Feb.
- [3] Luth, H. R.; Dallinga, R. P. (1999), "Prediction of Excessive Rolling of Cruise Vessels in Head and Following Waves". PRADS Conference.
- [4] Neves, M. A. S.; Pérez, N. A.; Valerio, L. (1999), "Stability of Small Fishing Vessels in Longitudinal Waves". Ocean Engineering, Vol. 26, No. 12.
- [5] Kerwin, J. E. (1955), "Notes on Rolling in Longitudinal Waves". International Shipbuilding Progress, No 16.
- [6] Paulling, J. R.; Rosenberg, R. M. (1959), "On Unstable Ship Motions Resulting from Non-linear Coupling". Journal of Ship Research, Vol. 3, No. 1.
- [7] Neves, M. A. S.; Valerio, L. (2000), "Parametric Resonance in Waves of Arbitrary Heading", VIth International Conference on Stability of Ships and Ocean Vehicles, STAB 2000, Launceston, Tasmania, Australia.
- [8] Himeno, Y. (1981), "Prediction of Ship Roll Damping - State of Art". Department of Naval Architecture and Marine Engineering, The University of Michigan. Report No 239.
- [9] Pérez, N.A.; Sanguinetti, C. F. O. (1995), "Experimental Results of Parametric Resonance Phenomenon of Roll Motion in Longitudinal Waves for Small Fishing Vessels". International Shipbuilding Progress, 42, No. 431, Sept.